

Parametric resonance of complex scalar field under spacetime oscillations

Shreyansh S. Dave¹ and Sanatan Digal^{1,2}

¹ The Institute of Mathematical Sciences, Chennai 600113, India,
shreyanshsd@imsc.res.in,

² Homi Bhabha National Institute, Training School Complex, Anushakti Nagar,
Mumbai 400085, India.

Abstract. In this proceeding, we study time evolution of a complex scalar field, in symmetry broken phase, in presence of oscillating spacetime metric background. We show that spacetime oscillations lead to parametric resonance of the field. This generates excitations in the field for a wide range of frequency of spacetime oscillations which ultimately lead to the formation of topological vortices. The lowest frequency cut-off to induce this phenomena is set by system size due to finite size effects.

Keywords: parametric resonance of classical field, topological vortices

1 Introduction

There are various systems ranging from condensed matter physics to the early Universe where topological defects can exist and form under various conditions [1]. They exist when the order parameter space or vacuum manifold of the system has a non-trivial topology [2]. Formation of topological defects during symmetry breaking phase transitions are studied by Kibble-Zurek mechanism [1,3]. Nucleation of superfluid vortex lattice in rotating vessel, flux-tube lattice in presence of magnetic field in type-II superconductor, etc. are other methods of formation of topological defects [4].

The phenomena of parametric resonance of field, in symmetry broken phase, can also produce topological defects [5,6,7]. This phenomena has been studied for periodically oscillating temperature of heat-bath, which generates excitations in the field leading to the formation of topological defects [5,6]. In ref.[7], we have shown that spacetime oscillations can also induce such phenomena for a wide range of frequencies. At frequencies lesser than the mass of field mainly transverse excitation of the field arises, while at higher frequencies longitudinal excitation also gets generated dominantly. In this case, the lowest frequency cut-off to generate field excitation is set by system size due to finite size effects. In this proceeding, we present some of the results of our work in ref.[7].

2 Equation of Motion

For simplicity, we take the *inverse* spacetime metric as, $g^{\mu\nu} \equiv \text{diag}(-1, 1-h, 1+h, 1)$, where $h \equiv h(t, z) = \varepsilon \sin(\omega(t-z))$; (t, x, y, z) are spacetime coordinates. The action

of a complex scalar field on this spacetime manifold is given by [7],

$$S = \int d^4x \sqrt{-g} \left[-\frac{1}{2} g^{\mu\nu} \partial_\mu \Phi^* \partial_\nu \Phi - V(\Phi^* \Phi) \right], \quad (1)$$

where, $g = \det(g_{\mu\nu}) = -(1-h^2)^{-1}$, $\Phi = \phi_1 + i\phi_2$, $\Phi^* = \phi_1 - i\phi_2$; ϕ_1 and ϕ_2 are real scalar fields. We consider symmetry breaking effective potential as,

$$V(\Phi^* \Phi) = \frac{\lambda}{4} (\Phi^* \Phi - \Phi_0^2)^2, \quad (2)$$

where, the mass of longitudinal-mode of field is $m_\Phi = \Phi_0 \sqrt{2\lambda}$. The equation of motion for (ϕ_1, ϕ_2) fields are [7],

$$\square \phi_i - \frac{dV}{d\phi_i} = 0; \quad \square \phi_i = \frac{1}{\sqrt{-g}} \partial_\mu (\sqrt{-g} g^{\mu\nu} \partial_\nu \phi_i); \quad i = 1, 2. \quad (3)$$

For the simplicity of solving it numerically, (i) we assume that there is no variation of the field Φ along z -direction, and (ii) we look at the solution of the field only in the $z=0$ plane. With these simplifications, the above equations in the expanded form become [7],

$$-\frac{1}{2} \frac{\varepsilon^2 \omega \sin(2\omega t)}{f(t)f(-t)} \frac{\partial \phi_i}{\partial t} - \frac{\partial^2 \phi_i}{\partial t^2} + f(t) \frac{\partial^2 \phi_i}{\partial x^2} + f(-t) \frac{\partial^2 \phi_i}{\partial y^2} - \lambda \phi_i (\phi_1^2 + \phi_2^2 - \Phi_0^2) = 0, \quad (4)$$

where, $f(t) = 1 - \varepsilon \sin(\omega t)$. These equations clearly indicate that spacetime oscillations can affect field evolution iff the initial field configuration has some fluctuations, which can naturally be present due to thermal and/or quantum fluctuations. The momentum of field-modes of initial field configuration get coupled with spacetime oscillations and by following resonance conditions undergo parametric resonant growths [7]. One can show that when $\omega < m_\Phi$, then mainly transverse excitation of the field arise, while when $\omega > m_\Phi$ along with transverse excitation, longitudinal excitation also gets generated dominantly [7].

3 Simulation details and results

In our simulations, we have considered only transverse fluctuations in the initial field configuration. With this initial field configuration, we solve Eq.4 by using second order Leapfrog method and by considering periodic boundary conditions along spatial directions. We use lattice spacing of $\Delta x = \Delta y = 0.01 \Lambda$ and evolve with time spacing of $\Delta t = 0.005 \Lambda$.

In Fig.1, we have shown how the field gets excitations under spacetime oscillations in physical space (left) and in field space (right) at four different times of field evolution; Left: $t=0, 1.35, 1.7,$ and 1.8Λ , Right: $t=0.05, 1.05, 1.35,$ and 1.8Λ . The parameters of simulations are $\varepsilon=0.4, \omega=100 \Lambda^{-1}, \Phi_0=10 \Lambda^{-1}$, and $\lambda=40$, which implies that for these parameters $\omega > m_\Phi$ allowing the dominant generation of longitudinal component of the field along with transverse component. Left

plots clearly show that due to spacetime oscillations, the field generates a specific field-modes at the intermediate stage of the evolution. With further evolution, other field-modes also get generated which ultimately lead to the formation of topological vortices in the system. Right plots show that both component of the field, transverse as well as longitudinal, have been generated during the field evolution. The generation of longitudinal excitation in this case makes the profile

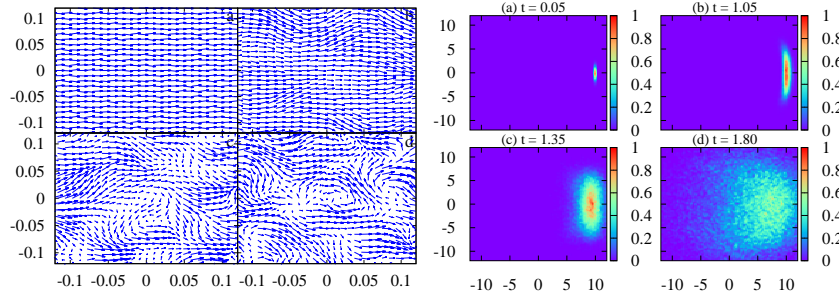


Fig. 1. Field configurations in physical space (left) and field distributions in field space (right) at different times of field evolution for $\omega > m_\phi$. Figures are from ref.[7].

of the formed vortices highly distorted. In Fig.2, we have taken $\omega = 20 \Lambda^{-1}$, for which $\omega < m_\phi$ allowing the generation of mainly transverse excitation. This leads to the formation of well separated vortices. This has been depicted in physical space (left) and in field space (right) at time $t = 18.5 \Lambda$.

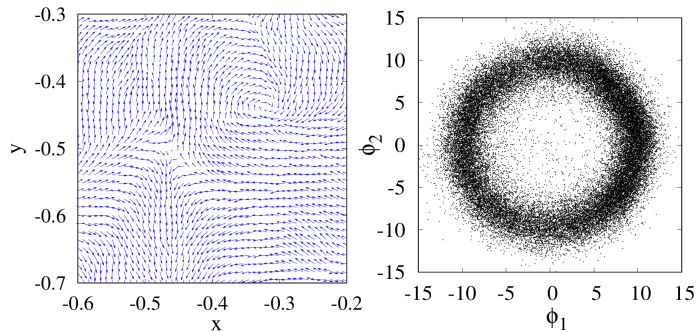


Fig. 2. Figures show formation of well separated vortices (left) and generation of mainly transverse excitation in field space (right) for $\omega < m_\phi$. Figures are from ref.[7].

In order to understand the response of field to frequency ω , we determine the time of formation of first vortex-antivortex pair in system and denote by t_{vortex} .

A more useful quantity to analyse this response is $t_{vortex} \omega/2\pi$, a dimensionless number, which counts the number of cycle (NoC) of spacetime oscillations up to t_{vortex} . In Fig.3 (left), we have plotted NoC versus ω . This clearly shows that for sufficiently large ω , NoC is almost independent from ω . However, at low ω , it starts deviating from such a constant value and diverges at very low ω . This is an indication of finite size effects. In Fig.3 (right), we have studied the effects of using periodic and fix boundary conditions (PBCs and FBCs), system size L , and ω on NoC. For each curve, we have taken fixed value of ω ($\omega_1=50 \text{ \AA}^{-1}$ and $\omega_2=100 \text{ \AA}^{-1}$), and $\varepsilon=0.4$, while we vary L . For sufficiently large values of $L\omega/4\pi$, NoC is independent from $L\omega/4\pi$ and takes roughly a constant value. On the other hand, for low $L\omega/4\pi$, it starts increasing and diversifies when $L\omega/4\pi \sim 1$. For PBCs these deviations are stronger than FBCs. Thus, the lowest frequency cut-off to induce this phenomenon is given by $\omega_L \sim 4\pi/L$.

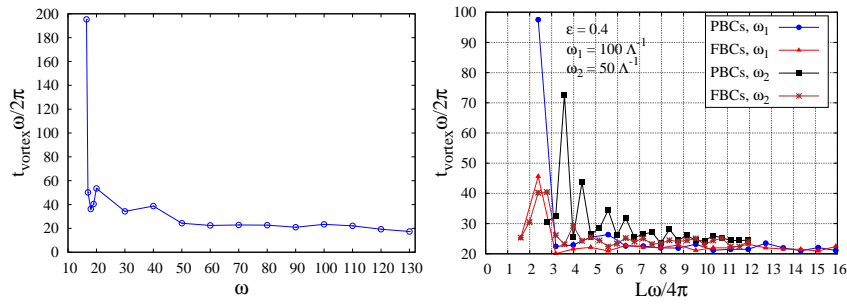


Fig. 3. Figures show response of t_{vortex} to frequency ω , choice of boundary conditions, and system size L . Figures are from ref.[7].

References

1. Zurek, W.H.: Cosmological experiments in condensed matter systems. Phys. Rep. 276, 177 (1996). doi:10.1016/S0370-1573(96)00009-9
2. Mermin, N.D.: The topological theory of defects in ordered media. Rev. Mod. Phys. 51, 591 (1979). doi:10.1103/RevModPhys.51.591
3. Kibble, T.W.B.: Topology of cosmic domains and strings. J. Phys. A 9, 1387 (1976). doi:10.1088/0305-4470/9/8/029
4. Tilley, D.R., Tilley, J.: Superfluidity and Superconductivity. Third Edition, Overseas Press (2005).
5. Digal, S., Ray, R., Sengupta, S., Srivastava, A.M.: Resonant Production of Topological Defects. Phys. Rev. Lett. 84, 826 (2000). doi:10.1103/PhysRevLett.84.826
6. Ray, R., Sengupta, S.: Stochastic production of kink-antikink pairs in the presence of an oscillating background. Phys. Rev. D 65, 063521 (2002). doi:10.1103/PhysRevD.65.063521
7. Dave, S.S., Digal, S.: Effects of oscillating spacetime metric background on a complex scalar field and formation of topological vortices. arXiv: 1911.13216 [hep-th].